
LocMoE+: Enhanced Router with Token Feature Awareness for Efficient LLM Pre-Training

Jing Li[†] Zhijie Sun^{†,*} Dachao Lin[†] Xuan He Yi Lin
Binfan Zheng Li Zeng Rongqian Zhao Xin Chen
Huawei Technologies Co., Ltd

{lijing473, sunzhijie3, lindachao1, hexuan22, linyi11}@huawei.com
{zhengbinfan1, zengli43, zhaorongqian, chenxin}@huawei.com

Abstract

Mixture-of-Experts (MoE) architectures have recently gained increasing popularity within the domain of large language models (LLMs) due to their ability to significantly reduce training and inference overhead. However, MoE architectures face challenges, such as significant disparities in the number of tokens assigned to each expert and a tendency toward homogenization among experts, which adversely affects the model's semantic generation capabilities. In this paper, we introduce LocMoE+, a refined version of the low-overhead LocMoE, incorporating the following enhancements: (1) Quantification and definition of the affinity between experts and tokens. (2) Implementation of a global-level adaptive routing strategy to rearrange tokens based on their affinity scores. (3) Reestimation of the lower bound for expert capacity, which has been shown to progressively decrease as the token feature distribution evolves. Experimental results demonstrate that, without compromising model convergence or efficacy, the number of tokens each expert processes can be reduced by over 60%. Combined with communication optimizations, this leads to an average improvement in training efficiency ranging from 5.4% to 46.6%. After fine-tuning, LocMoE+ exhibits a performance improvement of 9.7% to 14.1% across the GDAD, C-Eval, and TeleQnA datasets.

1 Introduction

Large language models (LLMs) have shown exceptional proficiency in understanding deep structures and complex semantic relationships within language [1]. As these models scale up, their capabilities in language generation and logical comprehension are enhanced, but this comes at the cost of significant computational, communication, and storage demands [2]. To scale models efficiently without disproportionately increasing computational costs, researchers have incorporated the Mixture-of-Experts (MoE) architecture into LLMs [3]. The MoE framework integrates multiple experts within the model, each tasked with processing specific types of inputs [4]. For a given input, only a subset of experts is activated, allowing for more efficient use of computational resources [5]. Recently, several LLMs employing MoE structures, such as DeepSeek-MoE [6] and Mixtral [7], have demonstrated outstanding performance on various leaderboards.

Despite the efficiency benefits of MoE in scaling model sizes, it introduces several new challenges and drawbacks [8]. For instance, an imbalanced "winner-takes-all" phenomenon among experts can detrimentally affect overall model performance [9], and the All-to-All communication pattern can become a bottleneck [10]. The model's convergence and the experts' generalization capabilities are heavily dependent on the design of the routing strategy. Recent research has addressed these challenges from multiple angles, such as optimizing routing strategies and enhancing communication efficiency. In terms of routing strategies, DeepSeek-MoE [6] introduced the concepts of vertical-class experts, created through fine-grained partitioning, and shared experts, which are always activated.

Google Brain proposed the Expert Choice (EC) routing algorithm [11], assigning experts with pre-determined buffer capacities to the Top-k tokens to ensure load balance. For communication efficiency, FastMoE [12] leverages Megatron-LM [13], a distributed training framework by NVIDIA, utilizing CUDA’s multi-stream mechanism to maximize the overlap between communication and computation. Tutel [14] introduced flexible All-to-All communication to alleviate throughput bottlenecks caused by smaller matrix dimensions and proposed 2DH All-to-All to align non-contiguous memory spaces and merge scattered communications. The uneven expert load in classical MoE [15] often necessitates token dropping or padding. Megablocks [16] employs block-sparse operations to overcome the limitations of dynamic routing, improving the balance between model quality and efficiency.

LocMoE [17] aims to enhance the interpretability of routing mechanisms while reducing computational and communication overhead. LocMoE leverages orthogonal routing weights to prevent token homogenization across different expert networks and introduces the Grouped Average Pooling (GrAP) layer [18] for token feature extraction. Under these conditions, LocMoE uses theoretical proofs to calculate the lower bound of expert capacity. Experimental results demonstrate that employing this lower bound does not degrade, but slightly enhances, performance on downstream tasks. Additionally, LocMoE introduces a loss regularization term that incorporates data locality and load balancing [19], leading to a 12% to 22% improvement in training efficiency.

Building on previous work, this paper proposes LocMoE+, which aims to further enhance training efficiency and model performance. LocMoE+ adopts GrAP and the locality loss regularization terms from LocMoE, and continues to analyze the impact of token features on expert selection. The primary contributions of this paper are as follows:

1. **The affinity score.** Given that expert selection is related to the angle between tokens and gating weights, the cosine similarity between tokens and gating weights is used to define the affinity score between tokens and experts. This score is utilized for token rearrangement and as a threshold for the lower bound of expert capacity.
2. **The hybrid token rearrangement scheme.** By integrating the concepts of Token Choice Router (TCR) and Expert Choice Router (ECR), the training success rate is enhanced while considering expert capacity constraints. Its effectiveness has been theoretically validated.
3. **The adaptive expert capacity.** Setting a holistic affinity threshold allows the lower bound of expert capacity to be significantly reduced. As training iterations increase, the information density of token features grows, causing the expert capacity to initially decrease and then stabilize, thereby enhancing training efficiency.

LocMoE+ uses the state-of-the-art MoE model Mixtral $8\times 7B$ as the backbone, and utilizes Ascend-Speed and ModelLink libraries for pre-training on Ascend NPU clusters. Experiments conducted on clusters with 32, 64, and 256 NPUs show that LocMoE+ improves training efficiency by 5.4% to 46.6% compared to the baseline, and by 2.9% to 13.3% compared to LocMoE. Model performance is enhanced by 9.7% to 14.1% compared to the baseline, and by 1.7% to 4.1% compared to LocMoE.

The rest of this paper is structured as follows: Section 2 introduces related work on LLMs, MoE, and the Ascend architecture. Section 3 reviews LocMoE and presents the methods proposed in this paper, along with theoretical evidence. Section 4 analyzes the experimental results of LocMoE+ regarding training efficiency and model performance. The final section summarizes the content of this paper and offers an outlook on future improvements.

2 Related Work

LLMs. BERT [20] and GPT [21] in 2018 marked the emergence of the LLM era. GPT-3 [22], with 175 billion parameters, demonstrated impressive capabilities in language understanding and generation in 2020. By 2023-2024, LLMs expanded to hundreds of billions to trillions of parameters: GPT-4 [23] achieved breakthroughs in zero-shot and few-shot learning; PaLM-2 [24] enhanced knowledge acquisition and reasoning; Chinchilla [25] optimized computational resources and model scale; and Claude-v1 [26] displayed a safer, human-aligned LLM. These LLMs have made significant advancements across domains, paving the way towards artificial general intelligence.

MoE. Despite the outstanding performance of LLMs in language understanding and generation, their high computational cost hinders further model scale expansion. To alleviate this issue, re-

searchers have introduced the MoE architecture, which incorporates multiple expert modules and dynamically selects a subset of experts to process inputs, significantly reducing computational overhead while maintaining performance. GShard [3] and Switch Transformer [4] employ Top-2 and Top-1 routing strategies, respectively, to mitigate the expert load imbalance problem. Hash Layer [27] adopt hashing techniques to simplify the gating mechanism and improve model performance. METRO [28] introduces a metric learning-based routing mechanism that guides expert selection by learning task-relevant metric functions, enhancing the model’s generalization ability. DSelect-k [29] proposes a dynamic selection algorithm based on Markov chains, adaptively choosing the number of experts to maintain performance while reducing training costs. Furthermore, DeepSpeed-MoE [30] optimizes expert parallelism and pipeline parallelism in MoE, further boosting training efficiency. These works lay the foundation for the subsequent application of MoE in LLMs.

Ascend Architecture. The AI Core in the Ascend 910B NPU adopts the DaVinci architecture [31], which is responsible for executing computation-intensive operators related to scalars, vectors, and 3D cubes, and is widely used in LLM training. Huawei’s proprietary cache coherence protocol interconnect, High Confidence Computing Systems (HCCS) [32], enables high-performance inter-device data communication in multi-card scenarios. The Huawei Collective Communication Library (HCCL) [33], designed for the Ascend processor, offers high-performance primitives for single-node multi-card and multi-node multi-card collective communication. It implements collective communication functions on PCIe, HCCS, and RoCE high-speed links, facilitating distributed training. PyTorch [34], a widely adopted deep learning framework, is compatible with the Ascend NPU through the Ascend extension for PyTorch [35]. AscendSpeed, an acceleration library tailored for Ascend devices, focuses on parallel strategy partitioning for LLMs and aggregates results through collective communication. ModelLink, a training framework designed for LLMs, fully considers the characteristics of the Ascend NPU and implements features such as memory optimization, multi-dimensional parallelism, and adaptive data loading, further enhancing training performance.

3 Method

Notation. We denote vectors by lowercase bold letters (e.g., \mathbf{w} , \mathbf{x}), and matrices by capital bold letters (e.g., \mathbf{W} , \mathbf{X}). We let $\|\cdot\|$ be the ℓ_2 -norm for vectors, and denote $\text{Unif}(\mathcal{S}^{d-1})$ as the uniform distribution over the surface of d -dim unit sphere \mathcal{S}^{d-1} . We take $\mathbb{1}_A$ as the indicator function on event A , i.e., $\mathbb{1}_A = 1$ if event A happens, and 0 otherwise. We adopt $[n] = \{1, \dots, n\}$ and Top- ℓ (Bottom- ℓ) as the index sets of the top- ℓ (bottom- ℓ) values, and $:=$ as the definition notation. We use $\mathcal{O}(\cdot)$, $\Omega(\cdot)$, $\Theta(\cdot)$ and $\tilde{\mathcal{O}}(\cdot)$ notation to hide universal constants and log-factors.

3.1 Background

Main Principle. The MoE architecture, based on the Transformer framework, efficiently scales up model size with low computational overhead, benefiting from two primary structures: a sparse gating network for routing tokens and expert networks for processing specific token categories. The sparse gating network determines the expert to which a token will be sent.

We consider the supervised classification for brevity where the training samples are $\{(\mathbf{x}^{(i)}, y_i)\}_{i=1}^N \sim \mathcal{D}$. Each training sample $\mathbf{x}^\top = (\mathbf{x}_1^\top, \dots, \mathbf{x}_s^\top) \in \mathbb{R}^{sd}$ has s tokens with token feature $\mathbf{x}_i \in \mathbb{R}^d, \forall i \in [s]$, and label $y \in \mathbb{N}^+$. The objective is to learn the map of \mathbf{x} to the corresponding y . The general MoE structure are formulated as

$$\text{MoE}(\mathbf{x}) = \sum_{t=1}^s \sum_{i=1}^n G_i(\mathbf{x}_t) \cdot E_i(\mathbf{x}_t), \quad (1)$$

where n is the number of experts, $G(\mathbf{x}_t): \mathbb{R}^d \rightarrow \mathbb{R}^n$ is the gating (or router) weights of experts which maps the tokens of \mathbf{x}_t into the corresponding experts with weights, e.g., $G_i(\mathbf{x}) = \text{Softmax}(\mathbf{W}\mathbf{x} + \epsilon)$ where the softmax is applied to each row, and $E_i(\mathbf{x}_t): \mathbb{R}^d \rightarrow \mathbb{R}$ is the i -th expert network, e.g., simple MLP models, see [36] for current different router methods. Generally, $n \ll s$, which saves much computation compared to the dense structure.

Routing Strategy. There are two main router methods: hard router [36] which uses hard assignments between tokens and experts with sparse dispatch matrix, and soft router [37] which uses

weighted combinations of tokens. In this paper, we still focus on the first one, since the computation cost is much smaller than the soft ones.

The hard router also have two main choices: 1) Token Choice Router (**TCR**) [38, 11], which lets each token choose its *top-scored* experts; Taking Top1 routing as an example, it typically selects a linear layer to extract feature representations for different experts and then obtains the expert index with the highest routing probability through the gating function. 2) Expert Choice Router (**ECR**), which lets each expert choose its *top-scored* tokens. Moreover, to balance the budget of differnet experts, we will pre-define the **expert capacity** C of all experts in practice, namely, the maximum tokens sent to each expert.

Chocie of score. In this paper, we define the **score** of t -th token and i -th expert as $\delta_{ti} = \cos(\mathbf{x}_t, \mathbf{w}_i) := \mathbf{x}_t^\top \mathbf{w}_i / (\|\mathbf{x}_t\| \cdot \|\mathbf{w}_i\|)$, i.e., the cosine similarity between vectors \mathbf{x}_t and \mathbf{w}_i . The score is to decide the gating weight in router. For example, we can route t -th token to the experts of the top- ℓ indices in $(\delta_{t1}, \dots, \delta_{tn})$.

Chocie of capacity. In previous works, expert capacity C is calculated using a capacity factor, ensuring that the size of each expert’s token buffer remains consistent. The choice of capacity factor is currently based mainly on empirical knowledge; increasing the capacity factor allows for handling more tokens but reduces training efficiency.

TCR expression. First, given ℓ , we decide the candidate expert set for each token by the sort of scores:

$$\left(\tilde{I}_{t1}, \dots, \tilde{I}_{t\ell}\right) = \text{Top-}\ell\left(\{\delta_{t1}, \dots, \delta_{tn}\}\right), \tilde{I}_{tk} \in [n], \forall t \in [s], k \in [\ell]. \quad (2)$$

Second, we choose the first- C tokens (or all if less than C) to each expert due to the capacity limit:

$$\left(I_{1i}, \dots, I_{Ci}\right) = \text{Bottom-}C\left(\left\{t \in [s] : \exists j \in [\ell], \tilde{I}_{tj} = i\right\}\right), I_{ki} \in [s] \cup \text{None}, \forall i \in [n], k \in [C]. \quad (3)$$

In practice, we adopt $\ell = 1$ to further save the computation cost since $n \ll s$.

ECR expression. We directly choose the tokens in the top- C scores of each expert:

$$\left(I_{1i}, \dots, I_{Ci}\right) = \text{Top-}C\left(\{\delta_{1i}, \dots, \delta_{si}\}\right), I_{ki} \in [s], \forall i \in [n], k \in [C]. \quad (4)$$

Intuitively, TCR can result in underused experts with fewer tokens than their allowed capacity, while ECR can result in underused tokens where no expert receives such token.

Auxiliary Loss. Feed-forward network (FFN) layers are commonly employed in expert networks, allowing each expert to learn independently as a separate neural network, thus preventing interference between samples. This mechanism leads to a severe load imbalance, as experts frequently selected in the early stages are more likely to be chosen in later stages. To mitigate this skewness in token allocation, the auxiliary loss [8] has been proposed, defined as $L_{\text{aux}} = \alpha n \sum_{i=1}^n f_i P_i$, where $f_i = \frac{1}{T} \sum_{\mathbf{x} \in \beta} \mathbb{1}_{\arg \max p(\mathbf{x}) = i}$, and $P_i = \frac{1}{T} \sum_{\mathbf{x} \in \beta} p_i(\mathbf{x})$. Here, β represents the batch containing T tokens, and p_i denotes the probability of a token being routed to expert i .

3.2 LocMoE

GrAP. In the work of LocMoE [17], the main idea is to enhance the differentiation of token features by orthogonalizing the gating weights. Consequently, LocMoE proposes a GrAP, supposing $n|d$ and $p := d/n \in \mathbb{N}^+$, the GrAP operator pooling every s dimensions to obtain the router score: $\text{GrAP}(\mathbf{x})^\top := \left(\frac{1}{p} \sum_{i=1}^p x_i, \dots, \frac{1}{p} \sum_{i=1}^p x_{jp+i}, \dots, \frac{1}{p} \sum_{i=1}^p x_{(n-1)p+i}\right) \in \mathbb{R}^n$. Specifically, the weight for each expert is represented as $\text{GrAP}(\mathbf{x})^\top = (\mathbf{w}_1^\top \mathbf{x} \cdots \mathbf{w}_n^\top \mathbf{x})$, with $\mathbf{w}_i := \underbrace{(\mathbf{0}_p \cdots \mathbf{0}_p)}_{i-1} \mathbf{1}_p \mathbf{0}_p \cdots \mathbf{0}_p)^\top, \forall i \in [n]$, leading to $\mathbf{w}_i \perp \mathbf{w}_j, \forall i \neq j \in [n]$.

The Lower Bound of the Expert Capacity. Under the premises of orthogonal gating weights and a data distribution approaching uniformity, LocMoE demonstrates that the expert capacity is closely related to the angle between the gating weights and tokens. For large scale of the activation, the lower bound of expert capacity is proven to exist and is represented as $C_{\min} = \frac{1}{n} \exp\{d\delta_{\max}^2 / (2 - \delta_{\max}^2)\}$.

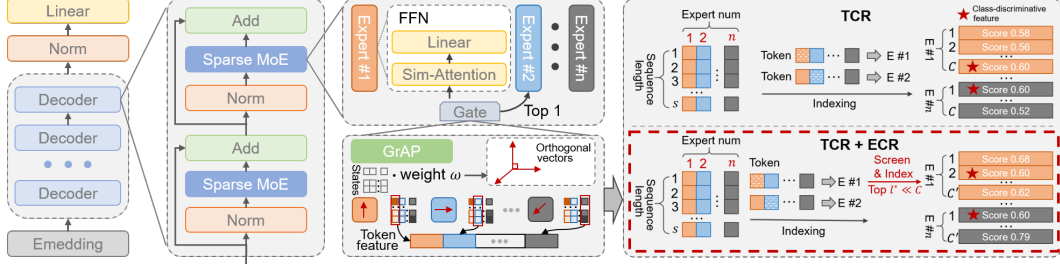


Figure 1: The architecture of the model along with the hybrid TCR+ECR router.

Locality Loss. Building upon the auxiliary loss, LocMoE introduces a loss bias term based on data locality, represented as $L_{loc} = \mu \text{KL}(D_c || D_1) = -\mu \int D_c(x) \ln \left[\frac{D_1(x)}{D_c(x)} \right] dx$, i.e., the Kullback-Leibler (KL) divergence of the current distribution $D_c(x)$ and the fully localized distribution $D_1(x)$. This loss term serves as a soft constraint, encouraging tokens to be sent to experts residing on the same node, thereby mitigating the substantial overhead incurred by partial inter-node communication.

3.3 Token Awareness Router for LocMoE

3.3.1 Scheme Sketch

Figure 1 illustrates the model constructed in this paper, with a particular focus on the proposed token awareness router. The model framework is GPT-like, comprising only decoders, and incorporates LocMoE+ in place of the gated routing of sparse MoE blocks. To enhance interpretability and reduce computational overhead, the original Top-2 routing is simplified to the sparsest Top-1 routing. Consequently, the weights of GrAP, consisting of orthogonal vectors, emphasize different aspects of token features, which are evenly divided and non-overlapping. This routing mechanism can be viewed as a multi-classification of these feature fragments.

TCR, introduced in the background, is exemplified in the figure. If the feature fragment corresponding to the k -th dimension of the gating weight for a particular token is more prominent, then that token will be routed to the k -th expert. If among all tokens routed to the k -th expert, there is a certain probability of the presence of class-discriminative tokens, then the capacity C must be set to a larger value to ensure the inclusion of sufficient class-discriminative tokens. The router proposed in this paper is a hybrid of TCR and ECR modes. After determining the expert to which a token will be routed, scores are calculated for the tokens assigned to each expert, and a Top- ℓ selection is performed, where ℓ^* is determined by a threshold of the sum of scores. Subsequent theoretical analysis will demonstrate the effectiveness of this hybrid routing scheme.

3.3.2 Theoretical Explanation

To explain the motivation of our method, we show some theoretical insights in this section. Our theoretical analysis is built on [39], where they assume the training data has unique class-discriminative patterns with exactly the same number as experts, and other class-irrelevant patterns. Chowdhury et al. [39] demonstrated that the classical MoE structure goes through two phases:

Phase 1: Router training ([39, Lemma 4.1, Assumption 4.4]), which makes class-discriminative patterns all go to the corresponding expert. This process ensures that each expert only receives the class-discriminative tokens related to the specific class.

Phase 2: Expert training ([39, Theorem 4.2, Theorem 4.5]), which makes each expert learn to predict the label based on its class-discriminative inputs from Phase 1. This process is designed to establish each expert's ability to handle and solve problems.

Hence, the training of an input in the current step is valid if the class-discriminative patterns are correctly dispatched. We compute **training success rate** of input (i.e., the probability of the tokens in an input being correctly dispatched to experts) to measure the difference between TCR and ECR,

We follow the setup in [39] that the input $x \in \mathbb{R}^{sd}$ with s tokens is comprised of one class-discriminative pattern $\mathbf{o}_1, \dots, \mathbf{o}_n \in \mathbb{R}^d$, with each deciding the label $y \in [n]$, and $s-1$ class-irrelevant

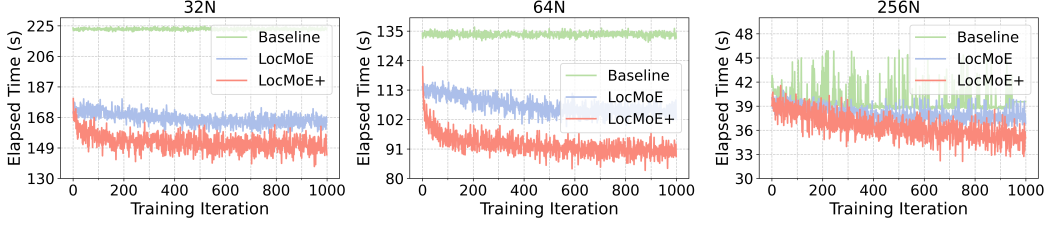


Figure 2: The time consumption during training iterations with different schemes and cluster sizes.

patterns $\mathbf{r} \sim \mathcal{N}$ (the distribution will be clarified below). To show the quantitative comparison of TCR and ECR in training success rate, we need following assumptions of token patterns.

Assumption 3.1 (class-discriminative). *We assume the location and feature of class-discriminative pattern is uniformly distribute in $[s]$ and $[n]$, i.e.,*

$$i \sim \text{Unif}([s]), \mathbf{x}_i \sim \text{Unif}(\{\mathbf{o}_1, \dots, \mathbf{o}_n\}).$$

We also assume that $\forall i \in [n], \mathbf{o}_i$ should be sent to the i -th expert, and define the true positive probability in token choice setting is no worse than the uniform dispatch as below

$$\mathbb{P}(\mathbf{o}_i \text{ sent to expert } i) = p_i \geq 1/n, \forall i \in [n].$$

Assumption 3.2 (class-irrelevant). *The distribution of class-irrelevant patterns is isotropy, i.e.,*

$$\mathbb{P}(\mathbf{r} \sim \mathcal{N}, \mathbf{r} \text{ sent to expert } i) = 1/n, \forall i \in [n]. \quad (5)$$

And we define the false positive probability in expert choice setting as

$$\mathbb{P}(\mathbf{r} \sim \mathcal{N}, \text{ the score of } \mathbf{r} \text{ is larger than } \mathbf{o}_i \text{ for expert } i) = q_i, \forall i \in [n], \quad (6)$$

which measures the possibility that expert i chooses the wrong token \mathbf{r} instead of the correct token \mathbf{o}_i .

Assumption 3.1 assumes the valid token is uniformly distributed in training samples due to the massive amounts of data nowadays. Assumption 3.2 assumes the invalid tokens can be uniformly dispatched to experts since the invalid tokens do not provide supervised signal to router and experts in training. We consider such uniform settings are common assumptions in theoretical analysis.

Now we compute the training success rate of TCR and ECR.

Theorem 3.3. *Under Assumptions 3.1 and 3.2, the training success rate of TCR in each sample \mathbf{x} is*

$$\mathbb{P}(\mathbf{x} \text{ succeed in TCR training}) = \Theta\left(C \sum_{i=1}^n p_i/s\right), \quad (7)$$

and the training success rate of ECR in each sample \mathbf{x} is

$$\mathbb{P}(\mathbf{x} \text{ succeed in ECR training}) \begin{cases} \leq \frac{1}{n} \sum_{i=1}^n e^{-(s-1)q_i/8}, & \text{if } C \leq (s-1)q_i/2 + 1, \forall i \in [n], \\ \geq 1 - e^{-3C/16}, & \text{if } C \geq 2(s-1)q_i, \forall i \in [n]. \end{cases} \quad (8)$$

Remark 3.4. *In practice, we have constant number of experts [7], i.e., $n = \Theta(1)$, and $C < s$ to save computation cost. We explain the benefit of swiching TCR to ECR during training based on Theorem 3.3 and feature distrution during training.*

At the beginning of training, the model seldom learn the task. Then the feature of class-irrelevant tokens is nearly isotropy, e.g., uniformly distrbute around the sphere (see Appendix B), leading to $q_i = \Theta(1)$. The succed rate of TCR with the form C/s is better than ECR with the form e^{-s} . Thus we should choose TCR with a large capacity $C = \Theta(s)$ to improve the success rate of training samples.

After training for some iterations, the experts can roughly distinguish the class-irrelevant and discriminative patterns, leading to $q_i \ll 1$ or $sq_i \leq C^$ for some $C^* > 0$ (see Appendix B). Then ECR with success rate nearly 1 is better than TCR with the form C/s as long as $C \geq 2C^*$. Thus we should choose ECR with a small capacity $C = \Theta(1)$ to improve the success rate of training samples.*

Indeed, we find that Chowdhury et al. [39, the definition of ℓ^] consider the ECR setting and verify the benefit in sample complexity. They assume the maximum number of class-irrelevant patches that are close to class-discriminative patches are bounded, which has similar effect as C^* in our scene.*

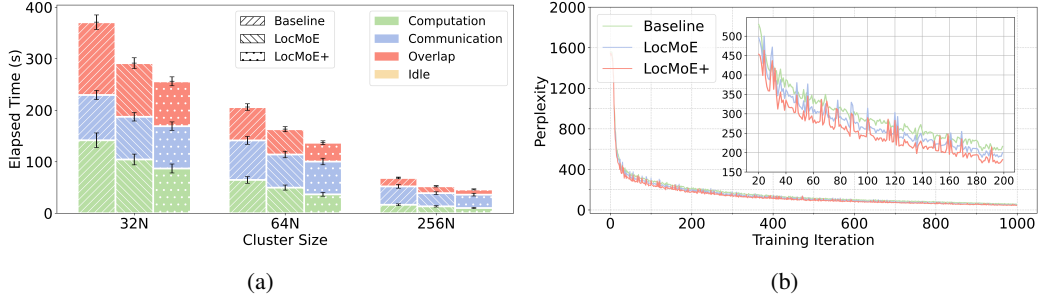


Figure 3: (a) The average composition of computation, communication, overlap, and idle with different schemes and cluster sizes. (b) The perplexity during training iterations with different schemes.

3.4 Communication Optimization

The training framework employs the Communication Over Computation (CoC) optimization technique to address performance bottlenecks in LLM training. During forward propagation in LLMs, the ColumnParallelLinear and RowParallelLinear components involve sequentially dependent computation (matrix multiplication) and communication (collective operations like AllReduce, AllGather, and ReduceScatter). These dependencies lead to inefficient serial execution. CoC decomposes these tasks into finer-grained subtasks and merges computation and communication into single kernels, such as MATMUL_ALL_REDUCE and MATMUL_REDUCE_SCATTER, utilizing MTE’s remote memory access capabilities. This approach allows for pipeline-style parallel execution and overlapping of computation and communication, significantly enhancing overall efficiency.

4 Experiments

4.1 Experimental Setup

The details of experimental setup including datasets, environment, configuration, and metrics, can be seen in Appendix C.

4.2 Efficiency Promotion and Memory Footprint Reduction

As detailed in Section 3, we consistently use Top-1 routing to ensure the routing implementation aligns with our theoretical framework. The Baseline model utilizes a limited expert capacity mode instead of the *groupedGEMM* scheme, which avoids token dropping, with the capacity factor set to 1.1. LocMoE considers data distribution uniformity and estimates expert capacity using a lower bound formula derived from its theoretical conclusions in the first batch, maintaining it as a constant during subsequent training. LocMoE+ fixes the range of score sums, processes hidden states, and calculates current expert capacity. The subsequent analysis addresses the training time, convergence, and memory usage efficiency of these schemes on multiple sizes of Ascend clusters.

Figure 2 illustrates the time consumption of these methods during the first 1000 iterations of training. Due to initialization and some unstable factors, time consumption is recorded starting from the 5th iteration. The Baseline model’s time consumption is relatively stable. As iterations increase, LocMoE’s time consumption slightly decreases, particularly in 32N and 64N, consistent with the conclusion that locality loss is effective only when the number of experts is greater than or equal to the number of nodes. LocMoE+ incurs slightly higher time consumption than LocMoE due to the computational overhead of token rearrangement. However, as token features converge, the required tokens gradually decrease and stabilize, leading to a decline in time consumption, which remains stable in subsequent training processes. Overall, LocMoE+ reduces training time by 2.9% to 13.3% compared to LocMoE, and by 5.4% to 46.6% compared to the Baseline.

We select 10 iterations at equal intervals from the training iterations to collect data on the time consumption of computation, communication, overlap, and idle periods, as shown in Figure 3a. It is important to note that the data collection operation also introduces some overhead. After integrating

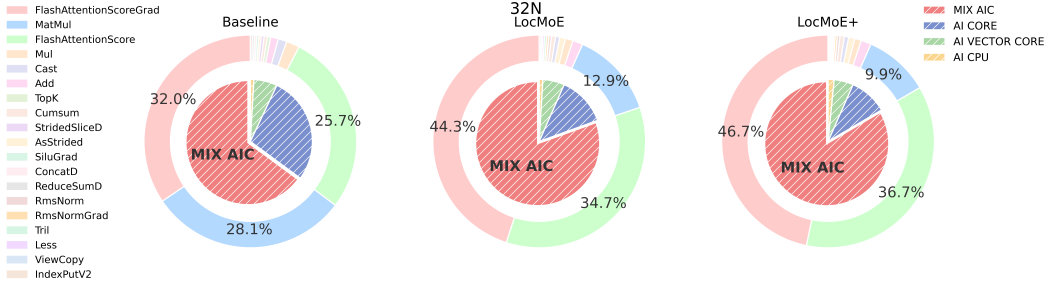


Figure 4: The distribution of time consumption for operators.

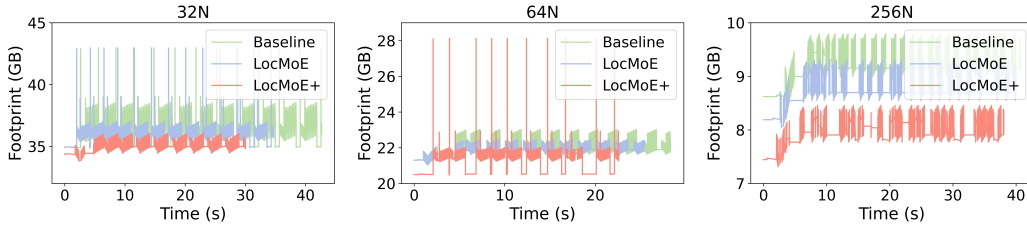


Figure 5: The footprint recorded in one acquisition cycle with different schemes and cluster sizes.

LocMoE and LocMoE+, the time consumption of each component decreases, with a significantly greater reduction in computation overhead compared to communication overhead. Additionally, as the cluster size increases, the proportion of computation/communication overlap decreases, and the magnitude of the reduction in computation overhead diminishes. Figure 3b illustrates perplexity as a measure of convergence. The convergence curves of these approaches indicate normal loss convergence, with LocMoE+ not adversely impacting convergence.

The proportional time consumption at the operator level is depicted in Figure 4. Among the components, AI CORE efficiently executes matrix multiplications and convolutions in AI algorithms; AI VECTOR CORE accelerates vector operations through parallel processing; MIX AIC integrates different types of operators and optimizes for multiple tasks; AI CPU is optimized in hardware and instruction sets to better support AI algorithms. LocMoE+ selects fewer tokens, resulting in a $17\times$ performance improvement in the FFN *MatMul* operator compared to the Baseline and a $2.6\times$ improvement compared to LocMoE. This leads to an overall $2.8\times$ reduction in the cumulative time consumption of the *MatMul* operator and a $2.6\times$ decrease in Cube computing load. However, the proportions of *TopK* and *IndexPutV2*, related to rearrangement, show a slight increase.

We select a single iteration during the stable training period and describe the per-device memory usage (Allocated) using the first 100,000 samples from its memory monitoring, as shown in Figure 5. Overall, LocMoE+ achieves memory usage reduction of 4.57% to 16.27% compared to the Baseline and 2.86% to 10.5% compared to LocMoE. As cluster size increases, the proportion of computational overhead decreases, and the gap in memory usage narrows. Additionally, instantaneous memory peaks gradually disappear, and the fluctuation amplitude of short-term memory also diminishes.

4.3 The Performance of Downstream Tasks

To enhance the model’s conversational capabilities and adaptability to downstream task, we fine-tuned the pre-trained models. As shown in Figure 6, with sufficient supervised fine-tuning (SFT), LocMoE+ achieves an average improvement of approximately 20.1% in 16 sub-capabilities of *Domain Task Capability*, which is a portion of General and Domain-specific Assessment Dataset (GDAD), compared to the Baseline, and an increase of about 3.5% compared to LocMoE. The *Rewriting* and *Summary* capabilities show the highest improvement, with a 28.2% increase compared to the Baseline and a 6.7% increase compared to LocMoE. In the 13 tests of *Domain Competency Exam*, LocMoE+ demonstrates an average improvement of 16% relative to the Baseline and an average increase of approximately 4.8% compared to LocMoE. The *IP Training* in the digital communications domain shows the most significant improvement, with a 27.3% increase compared to the Baseline and a 3.0%

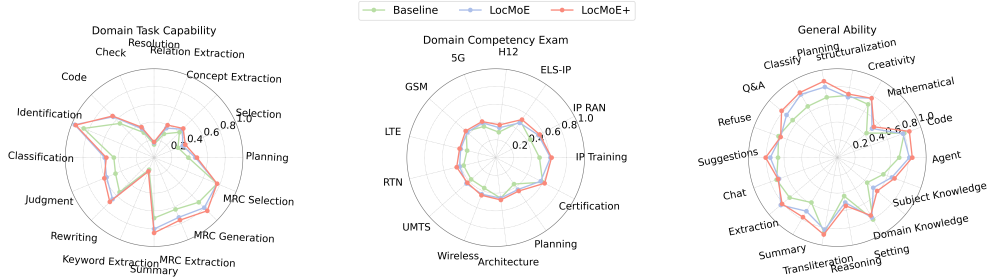


Figure 6: The performance on three categories of GDAD.

Table 1: Performance promotion obtained by LocMoE+ on different datasets.

	GDAD					
	GDAD-1	GDAD-2	GDAD-3	Avg	C-Eval	TeleQnA
Baseline	47.8	43.0	65.4	52.8	38.5	62.1
LocMoE	55.5	47.6	71.1	59.0	42.6	67.6
LocMoE+	57.4	49.9	74.5	61.5	43.1	68.8

increase compared to LocMoE. Among the 18 sub-capabilities of *General Ability*, LocMoE+ exhibits an improvement of about 13.9% relative to the Baseline and an average increase of 4.8% compared to LocMoE. The capability of *Planning* demonstrates the highest improvement, with a 26.8% increase compared to the Baseline and a 2.92% increase compared to LocMoE.

Table 1 presents the holistic evaluation results for multiple datasets, where GDAD-1 represents *Domain Task Capability*, and the other metrics follow accordingly. Notably, due to the 6:4 ratio of Chinese to English data in our incremental pre-training domain data and the 7:3 ratio in the fine-tuning data, LocMoE+ achieves an improvement of approximately 10.7% compared to the Baseline and 1.2% compared to LocMoE in the C-Eval [40] evaluation, despite the limited data available for training. During incremental training and fine-tuning, we incorporated substantial telecommunications domain knowledge, questions, and case studies. TeleQnA [41], the first benchmark dataset designed to evaluate the knowledge of LLMs in telecommunications, effectively measures the model’s capabilities in this domain. Consequently, LocMoE+ comprehensively surpasses both the Baseline and LocMoE on this specific dataset.

5 Conclusion

In this paper, we propose a novel MoE structure incorporating token feature awareness mechanism to enhance the training efficiency and performance of LLMs. Building upon the feature extraction component and locality loss of LocMoE, LocMoE+ introduces a routing strategy that combines TCR and ECR, theoretically demonstrating improved training success rates. By defining the affinity between tokens and experts, expert capacity can be dynamically reduced and further minimized. Model training experiments are conducted on Ascend clusters, leveraging the communication optimization characteristics of CoC. LocMoE+ achieves performance improvements up to 46.6% (32N) compared to the Baseline and 13.3% (32N) compared to LocMoE, while reducing memory usage by up to 16.27% and 10.5%, respectively. To evaluate model performance, all pre-trained models are fine-tuned using a mixture of domain-specific and general data, and assessed with the open-source datasets C-Eval and TeleQnA, and closed domain benchmark GDAD. In downstream tasks, LocMoE+ outperforms the Baseline by 14.1%, 10.7%, and 9.7% on GDAD, C-Eval, and TeleQnA, respectively; it exceeds LocMoE by 4.1%, 1.2%, and 1.7% on these datasets, respectively. Both theoretical proofs and experimental results demonstrate the benefits of the LocMoE+ routing strategy for LLM training efficiency. Future work may explore methods to compress communication data to further reduce communication overhead.

References

- [1] Wayne Xin Zhao, Kun Zhou, Junyi Li, Tianyi Tang, Xiaolei Wang, Yupeng Hou, Yingqian Min, Beichen Zhang, Junjie Zhang, Zican Dong, et al. A survey of large language models. [arXiv preprint arXiv:2303.18223](#), 2023.
- [2] Ziheng Jiang, Haibin Lin, Yinmin Zhong, Qi Huang, Yangrui Chen, Zhi Zhang, Yanghua Peng, Xiang Li, Cong Xie, Shibiao Nong, et al. {MegaScale}: Scaling large language model training to more than 10,000 {GPUs}. In [21st USENIX Symposium on Networked Systems Design and Implementation \(NSDI 24\)](#), pages 745–760, 2024.
- [3] Dmitry Lepikhin, HyoukJoong Lee, Yuanzhong Xu, Dehao Chen, Orhan Firat, Yanping Huang, Maxim Krikun, Noam Shazeer, and Zhifeng Chen. Gshard: Scaling giant models with conditional computation and automatic sharding. [arXiv preprint arXiv:2006.16668](#), 2020.
- [4] William Fedus, Barret Zoph, and Noam Shazeer. Switch transformers: Scaling to trillion parameter models with simple and efficient sparsity. [Journal of Machine Learning Research](#), 23(120):1–39, 2022.
- [5] Nan Du, Yanping Huang, Andrew M Dai, Simon Tong, Dmitry Lepikhin, Yuanzhong Xu, Maxim Krikun, Yanqi Zhou, Adams Wei Yu, Orhan Firat, et al. Glam: Efficient scaling of language models with mixture-of-experts. In [International Conference on Machine Learning](#), pages 5547–5569. PMLR, 2022.
- [6] Damai Dai, Chengqi Deng, Chenggang Zhao, RX Xu, Huazuo Gao, Deli Chen, Jiashi Li, Wangding Zeng, Xingkai Yu, Y Wu, et al. Deepseekmoe: Towards ultimate expert specialization in mixture-of-experts language models. [arXiv preprint arXiv:2401.06066](#), 2024.
- [7] Albert Q Jiang, Alexandre Sablayrolles, Antoine Roux, Arthur Mensch, Blanche Savary, Chris Bamford, Devendra Singh Chaplot, Diego de las Casas, Emma Bou Hanna, Florian Bressand, et al. Mixtral of experts. [arXiv preprint arXiv:2401.04088](#), 2024.
- [8] Noam Shazeer, Azalia Mirhoseini, Krzysztof Maziarz, Andy Davis, Quoc Le, Geoffrey Hinton, and Jeff Dean. Outrageously large neural networks: The sparsely-gated mixture-of-experts layer. [arXiv preprint arXiv:1701.06538](#), 2017.
- [9] Jiamin Li, Yimin Jiang, Yibo Zhu, Cong Wang, and Hong Xu. Accelerating distributed {MoE} training and inference with lina. In [2023 USENIX Annual Technical Conference \(USENIX ATC 23\)](#), pages 945–959, 2023.
- [10] Chang Chen, Min Li, Zhihua Wu, Dianhai Yu, and Chao Yang. Ta-moe: Topology-aware large scale mixture-of-expert training. [Advances in Neural Information Processing Systems](#), 35:22173–22186, 2022.
- [11] Yanqi Zhou, Tao Lei, Hanxiao Liu, Nan Du, Yanping Huang, Vincent Zhao, Andrew M Dai, Quoc V Le, James Laudon, et al. Mixture-of-experts with expert choice routing. [Advances in Neural Information Processing Systems](#), 35:7103–7114, 2022.
- [12] Jiaao He, Jiezhong Qiu, Aohan Zeng, Zhilin Yang, Jidong Zhai, and Jie Tang. Fastmoe: A fast mixture-of-expert training system. [arXiv preprint arXiv:2103.13262](#), 2021.
- [13] Mohammad Shoeybi, Mostofa Patwary, Raul Puri, Patrick LeGresley, Jared Casper, and Bryan Catanzaro. Megatron-lm: Training multi-billion parameter language models using model parallelism. [arXiv preprint arXiv:1909.08053](#), 2019.
- [14] Changho Hwang, Wei Cui, Yifan Xiong, Ziyue Yang, Ze Liu, Han Hu, Zilong Wang, Rafael Salas, Jithin Jose, Prabhat Ram, et al. Tutel: Adaptive mixture-of-experts at scale. [Proceedings of Machine Learning and Systems](#), 5, 2023.
- [15] Xiaozhe Ren, Pingyi Zhou, Xinfan Meng, Xinjing Huang, Yadao Wang, Weichao Wang, Pengfei Li, Xiaoda Zhang, Alexander Podolskiy, Grigory Arshinov, et al. Pangu-{\Sigma}: Towards trillion parameter language model with sparse heterogeneous computing. [arXiv preprint arXiv:2303.10845](#), 2023.

- [16] Trevor Gale, Deepak Narayanan, Cliff Young, and Matei Zaharia. Megablocks: Efficient sparse training with mixture-of-experts. Proceedings of Machine Learning and Systems, 5, 2023.
- [17] Jing Li, Zhijie Sun, Xuan He, Li Zeng, Yi Lin, Entong Li, Binfan Zheng, Rongqian Zhao, and Xin Chen. Locmoe: A low-overhead moe for large language model training. arXiv preprint arXiv:2401.13920, 2024.
- [18] Xing Wang, Han Zhang, and Zhaohui Du. Multi-scale noise reduction attention network for aero-engine bearing fault diagnosis. IEEE Transactions on Instrumentation and Measurement, 2023.
- [19] Noam Shazeer, Youlong Cheng, Niki Parmar, Dustin Tran, Ashish Vaswani, Penporn Koanantakool, Peter Hawkins, HyoukJoong Lee, Mingsheng Hong, Cliff Young, et al. Mesh-tensorflow: Deep learning for supercomputers. Advances in neural information processing systems, 31, 2018.
- [20] Jacob Devlin Ming-Wei Chang Kenton and Lee Kristina Toutanova. Bert: Pre-training of deep bidirectional transformers for language understanding. In Proceedings of NAACL-HLT, pages 4171–4186, 2019.
- [21] Alec Radford, Karthik Narasimhan, Tim Salimans, Ilya Sutskever, et al. Improving language understanding by generative pre-training.
- [22] Luciano Floridi and Massimo Chiriatti. Gpt-3: Its nature, scope, limits, and consequences. Minds and Machines: Journal for Artificial Intelligence, Philosophy and Cognitive Science, 2020.
- [23] Josh Achiam, Steven Adler, Sandhini Agarwal, Lama Ahmad, Ilge Akkaya, Florencia Leoni Aleman, Diogo Almeida, Janko Altenschmidt, Sam Altman, Shyamal Anadkat, et al. Gpt-4 technical report. arXiv preprint arXiv:2303.08774, 2023.
- [24] Rohan Anil, Andrew M Dai, Orhan Firat, Melvin Johnson, Dmitry Lepikhin, Alexandre Passos, Siamak Shakeri, Emanuel Taropa, Paige Bailey, Zhifeng Chen, et al. Palm 2 technical report. arXiv preprint arXiv:2305.10403, 2023.
- [25] Jordan Hoffmann, Sebastian Borgeaud, Arthur Mensch, Elena Buchatskaya, Trevor Cai, Eliza Rutherford, Diego de Las Casas, Lisa Anne Hendricks, Johannes Welbl, Aidan Clark, et al. Training compute-optimal large language models. arXiv preprint arXiv:2203.15556, 2022.
- [26] Alexander Wei, Nika Haghtalab, and Jacob Steinhardt. Jailbroken: How does llm safety training fail? Advances in Neural Information Processing Systems, 36, 2024.
- [27] Stephen Roller, Sainbayar Sukhbaatar, Jason Weston, et al. Hash layers for large sparse models. Advances in Neural Information Processing Systems, 34:17555–17566, 2021.
- [28] Payal Bajaj, Chenyan Xiong, Guolin Ke, Xiaodong Liu, Di He, Saurabh Tiwary, Tie-Yan Liu, Paul Bennett, Xia Song, and Jianfeng Gao. Metro: Efficient denoising pretraining of large scale autoencoding language models with model generated signals. arXiv preprint arXiv:2204.06644, 2022.
- [29] Hussein Hazimeh, Zhe Zhao, Aakanksha Chowdhery, Maheswaran Sathiamoorthy, Yihua Chen, Rahul Mazumder, Lichan Hong, and Ed Chi. Dselect-k: Differentiable selection in the mixture of experts with applications to multi-task learning. Advances in Neural Information Processing Systems, 34:29335–29347, 2021.
- [30] Samyam Rajbhandari, Conglong Li, Zhewei Yao, Minjia Zhang, Reza Yazdani Aminabadi, Ammar Ahmad Awan, Jeff Rasley, and Yuxiong He. Deepspeed-moe: Advancing mixture-of-experts inference and training to power next-generation ai scale. In International conference on machine learning, pages 18332–18346. PMLR, 2022.
- [31] Yifeng Tang and Cho-li Wang. Performance modeling on davinci ai core. Journal of Parallel and Distributed Computing, 175:134–149, 2023.

- [32] Jing Xia, Chuanning Cheng, Xiping Zhou, Yuxing Hu, and Peter Chun. Kunpeng 920: The first 7-nm chiplet-based 64-core arm soc for cloud services. *IEEE Micro*, 41(5):67–75, 2021.
- [33] Zijian Cao, Qiao Sun, Wenhao Yang, Changcheng Song, Zhe Wang, and Huiyuan Li. A novel hpl-ai approach for fp16-only accelerator and its instantiation on kunpeng+ ascend ai-specific platform. *Journal of Parallel and Distributed Computing*, 190:104884, 2024.
- [34] Adam Paszke, Sam Gross, Francisco Massa, Adam Lerer, James Bradbury, Gregory Chanan, Trevor Killeen, Zeming Lin, Natalia Gimelshein, Luca Antiga, et al. Pytorch: An imperative style, high-performance deep learning library. *Advances in neural information processing systems*, 32, 2019.
- [35] Zeling Zhu, Bangchuan Wang, Chuying Yang, Rui Zhu, Mingyao Zhou, and Nenggan Zheng. Performance evaluation of mindspore and pytorch based on ascend npu. In *2023 IEEE 29th International Conference on Parallel and Distributed Systems (ICPADS)*, pages 1826–1832. IEEE, 2023.
- [36] Tianlin Liu, Mathieu Blondel, Carlos Riquelme, and Joan Puigcerver. Routers in vision mixture of experts: An empirical study. *arXiv preprint arXiv:2401.15969*, 2024.
- [37] Joan Puigcerver, Carlos Riquelme, Basil Mustafa, and Neil Houlsby. From sparse to soft mixtures of experts. *arXiv preprint arXiv:2308.00951*, 2023.
- [38] Aidan Clark, Diego de Las Casas, Aurelia Guy, Arthur Mensch, Michela Paganini, Jordan Hoffmann, Bogdan Damoc, Blake Hechtman, Trevor Cai, Sebastian Borgeaud, et al. Unified scaling laws for routed language models. In *International conference on machine learning*, pages 4057–4086. PMLR, 2022.
- [39] Mohammed Nowaz Rabbani Chowdhury, Shuai Zhang, Meng Wang, Sijia Liu, and Pin-Yu Chen. Patch-level routing in mixture-of-experts is provably sample-efficient for convolutional neural networks. In *International Conference on Machine Learning*, pages 6074–6114. PMLR, 2023.
- [40] Yuzhen Huang, Yuzhuo Bai, Zhihao Zhu, Junlei Zhang, Jinghan Zhang, Tangjun Su, Junteng Liu, Chuancheng Lv, Yikai Zhang, Yao Fu, et al. C-eval: A multi-level multi-discipline chinese evaluation suite for foundation models. *Advances in Neural Information Processing Systems*, 36, 2024.
- [41] Ali Maatouk, Fadhel Ayed, Nicola Piovesan, Antonio De Domenico, Merouane Debbah, and Zhi-Quan Luo. Teleqna: A benchmark dataset to assess large language models telecommunications knowledge. *arXiv preprint arXiv:2310.15051*, 2023.
- [42] Fan Chung and Linyuan Lu. Concentration inequalities and martingale inequalities: a survey. *Internet mathematics*, 3(1):79–127, 2006.

A Missing Proofs

A.1 Auxiliary Results

Lemma A.1 (Theorem 4 in [42]). *Let $\mathbf{X}_1, \dots, \mathbf{X}_n$ be n independent random variables with*

$$\mathbb{P}(\mathbf{X}_i = 1) = p_i, \mathbb{P}(\mathbf{X}_i = 0) = 1 - p_i.$$

We consider the sum $\mathbf{X} = \sum_{i=1}^n \mathbf{X}_i$, with expectation $\mathbb{E}(\mathbf{X}) = \sum_{i=1}^n p_i$. Then we have

$$\begin{aligned} \text{(Lower tail)} \quad \mathbb{P}(\mathbf{X} \leq \mathbb{E}\mathbf{X} - \lambda) &\leq e^{-\frac{\lambda^2}{2\mathbb{E}\mathbf{X}}}, \\ \text{(Upper tail)} \quad \mathbb{P}(\mathbf{X} \geq \mathbb{E}\mathbf{X} + \lambda) &\leq e^{-\frac{\lambda^2}{2(\mathbb{E}\mathbf{X} + \lambda/3)}}. \end{aligned} \tag{9}$$

A.2 Proof of Theorem 3.3

Proof. 1) For the TCR, denote $s_i = |\{t < k : \mathbf{x}_t \text{ sent to expert } i, \mathbf{x}_k = \mathbf{o}_i\}|, \forall i \in [n]$ as the top class-irrelevant token number candidate to the i -th expert before the valid token. Then by Assumption 3.2, each class-irrelevant token uniformly gives to any expert, leading to $s_i | (\mathbf{x}_k = \mathbf{o}_i) \sim \mathcal{B}(k-1, 1/n)$ (Binomial distribution), that is,

$$\mathbb{P}(s_i = t | \mathbf{x}_k = \mathbf{o}_i) = \binom{k-1}{t} \cdot \left(\frac{1}{n}\right)^t \left(1 - \frac{1}{n}\right)^{k-1-t}, \forall t \in [k-1].$$

Then we could derive that

$$\begin{aligned} \mathbb{P}(\mathbf{x} \text{ succeed in training}) &= \sum_{i=1}^n \mathbb{P}(\mathbf{o}_i \text{ sent to expert } i | \mathbf{o}_i \text{ is in } \mathbf{x}) \mathbb{P}(\mathbf{o}_i \text{ is in } \mathbf{x}) \\ &= \frac{1}{ns} \sum_{i=1}^n \sum_{k=1}^s p_i \mathbb{P}(s_i < C | \mathbf{x}_k = \mathbf{o}_i) = \frac{1}{ns} \sum_{i=1}^n p_i \left(C + \sum_{k=C+1}^s \mathbb{P}(s_i < C | \mathbf{x}_k = \mathbf{o}_i) \right). \end{aligned} \tag{10}$$

Note that $\mathbb{E}s_i = (k-1)/n$. When $k \geq 2nC$, by lower tail bound in Lemma A.1, we get

$$\mathbb{P}(s_i < C | \mathbf{x}_k = \mathbf{o}_i) \leq e^{-\frac{(k-1-n(C-1))^2}{2(k-1)n}} \leq e^{-\frac{k-1}{8n}}.$$

Hence, we get the upper bound that

$$\begin{aligned} \mathbb{P}(\mathbf{x} \text{ succeed in training}) &\stackrel{(10)}{\leq} \frac{1}{ns} \sum_{i=1}^n \sum_{k=1}^s p_i \mathbb{P}(s_i < C | \mathbf{x}_k = \mathbf{o}_i) \\ &= \frac{1}{ns} \sum_{i=1}^n p_i \left(2nC + \sum_{k=2nC+1}^s \mathbb{P}(s_i < C | \mathbf{x}_k = \mathbf{o}_i) \right) \\ &\leq \frac{1}{ns} \sum_{i=1}^n p_i \left(2nC + \sum_{k=2nC}^{s-1} e^{-\frac{k}{8n}} \right) \leq \frac{1}{ns} \sum_{i=1}^n p_i \left(2nC + \frac{e^{-\frac{C}{4}}}{1 - e^{-\frac{1}{8n}}} \right) \\ &\stackrel{(i)}{\leq} \frac{1}{ns} \sum_{i=1}^n p_i \left(2nC + (8n+1)e^{-\frac{C}{4}} \right) \leq \frac{10C \sum_{i=1}^n p_i}{s}, \end{aligned} \tag{11}$$

where (i) uses the inequality that $e^{-t} \leq 1/(1+t), \forall t \geq 0$.

Moreover, for $1 + \frac{nC}{4} \leq k \leq 1 + \frac{nC}{2}$, i.e., $2(k-1) \leq nC \leq 4(k-1)$, by upper tail bound in Lemma A.1, we get

$$\mathbb{P}(s_i < C | \mathbf{x}_k = \mathbf{o}_i) = 1 - \mathbb{P}(s_i \geq C | \mathbf{x}_k = \mathbf{o}_i) \geq 1 - e^{-\frac{3(nC-k+1)^2}{2n[2(k-1)+nC]}} \geq 1 - e^{-\frac{k-1}{4n}}.$$

Hence, we get the lower bound that

$$\begin{aligned}
\mathbb{P}(\mathbf{x} \text{ succeed in training}) &\stackrel{(10)}{\geq} \frac{1}{ns} \sum_{i=1}^n \sum_{k=1}^s p_i \mathbb{P}(s_i < C | \mathbf{x}_k = \mathbf{o}_i) \\
&= \frac{1}{ns} \sum_{i=1}^n p_i \left(\sum_{k=\lceil 1+nC/4 \rceil}^{\lfloor 1+nC/2 \rfloor} \mathbb{P}(s_i < C | \mathbf{x}_k = \mathbf{o}_i) \right) \\
&\geq \frac{1}{ns} \sum_{i=1}^n p_i \left(\frac{nC}{4} - 1 - \sum_{k=\lceil 1+nC/4 \rceil}^{\lfloor 1+nC/2 \rfloor} e^{-\frac{k-1}{4n}} \right) \geq \frac{1}{ns} \sum_{i=1}^n p_i \left(\frac{nC}{4} - 1 - \frac{e^{-\frac{C}{16}}}{1 - e^{-\frac{1}{4n}}} \right) \\
&\stackrel{(i)}{\geq} \frac{1}{ns} \sum_{i=1}^n p_i \left(\frac{nC}{4} - 2 - (4n+1)e^{-\frac{C}{16}} \right) \geq \frac{C \sum_{i=1}^n p_i}{5s},
\end{aligned} \tag{12}$$

where (i) uses the inequality that $e^{-t} \leq 1/(1+t)$, $\forall t \geq 0$, and the final inequality needs $C \geq 48$, which can be satisfied in common experiments. Combining the upper and lower bounds, we obtain the desired result.

2) For the ECR, denote s_i as the class-irrelevant token number with the score larger than \mathbf{o}_i for i -th expert. By Assumption 3.2, we derive that $s_i \sim \mathcal{B}(s-1, q_i)$, $\forall i \in [n]$.

$$\begin{aligned}
\mathbb{P}(\mathbf{x} \text{ succeed in training}) &= \sum_{i=1}^n \mathbb{P}(\text{expert } i \text{ choose } \mathbf{o}_i | \mathbf{o}_i \text{ is in } \mathbf{x}) \mathbb{P}(\mathbf{o}_i \text{ is in } \mathbf{x}) \\
&= \frac{1}{n} \sum_{i=1}^n \mathbb{P}(s_i \leq C-1, s_i \sim \mathcal{B}(s-1, q_i))
\end{aligned} \tag{13}$$

If $C-1 \leq (s-1)q_i/2$, by lower tail bound in Lemma A.1 with $\lambda = (s-1)q_i - (C-1) < \mathbb{E}s_i$, we obtain that

$$\mathbb{P}(s_i \leq C-1) \leq e^{-\frac{(s-1)q_i}{2} \left(1 - \frac{C-1}{(s-1)q_i}\right)^2} \leq e^{-\frac{(s-1)q_i}{8}}.$$

If $C \geq 2(s-1)q_i$, by upper tail bound in Lemma A.1 with $\lambda = C - (s-1)q_i > 0$, we obtain that

$$\mathbb{P}(s_i \leq C-1) = 1 - \mathbb{P}(s_i \geq C) \geq 1 - e^{-\frac{[C-(s-1)q_i]^2}{2(C+2(s-1)q_i)^3}} \geq 1 - e^{-\frac{3C}{16}}.$$

Hence, we conclude Eq. (8). \square

B Token Feature Distribution

We also validate the feature distribution before and after MoE training shown in Figure 7. We can see before training, all 8192 tokens in one training sample are nearly orthogonal with correlation coefficient near zero, which verifies the isotropy distribution assumption in the first bullet of Remark 3.4. After training, the token features are nearly aligned with correlation coefficient large than 0.8. We can also observe that neighbouring tokens share similar features, and clear block feature behavior, meaning that the token features are relatively separated and the number of tokens in each cluster is bounded, which somehow matches the distribution assumption in the second bullet of Remark 3.4.

C Experimental Setup

C.1 Datasets for Training and Fine-Tuning

The dataset used in this paper is a self-constructed dataset that integrates knowledge from multiple domains, including wireless, data communication, and cloud-core technologies. It comprises Chinese, English, and bilingual corpora. The corpora are parsed from various internal technical documents, such as iCase, blogs, Wiki, and feature documents. Taking iCase as an example, iCase is a case record of problem localization and handling processes, containing code, instructions, and corresponding logs. In addition, the above-mentioned domain-specific knowledge corpora are mixed with general corpora in a ratio of 1:5. The general corpora are collected from hundreds of websites, including online novels,

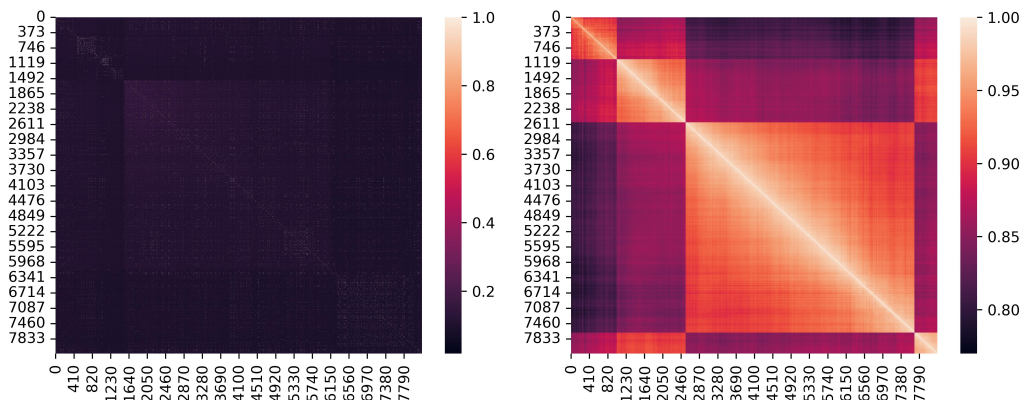


Figure 7: The correlation matrix of one training sample feature before (left) and after (right) training.

cooking guides, movie reviews, and more. After cleaning, deduplication, and review operations, the dataset is thoroughly shuffled. A total of 4.19 billion tokens is sampled as the experimental pre-training dataset. To evaluate downstream tasks, this paper also adopt hybrid sft data items to fine-tune the pre-trained model. The dataset comprises 762,321 general question-answer pairs and 11,048 domain-specific question-answer pairs, with a general-to-domain ratio of 68:1. The general characteristics encompass multi-tasking, mathematical ability, coding ability, logical reasoning, multi-turn dialogue, knowledge reasoning, language understanding, text generation, multi-tasking, FunctionCall, CoT, MRC summarization, refusal to answer, Chinese, and English. The domain-specific characteristics include domain knowledge understanding, RAG, FunctionCall, information extraction, multi-turn dialogue, reading comprehension, paraphrasing, and intent recognition.

C.2 Experimental Environment

The experiments are conducted on a cluster composed of Ascend 910B3 NPUs, divided into three groups: 32 NPUs (hereinafter referred to as 32N, and so on), 64N, and 256N. The 910B3 series NPU contains 20 AI cores with a main frequency of 1.8GHz and a theoretical computing power of 313T under fp16 precision. The physical High Bandwidth Memory (HBM) of the 910B3 NPU is 64G, with an HBM frequency of 1.6GHz and an HBM bandwidth of 1.6T. Every 8 NPUs are mounted on the same Atlas 800T A2 server, which internally adopts a fullmesh networking scheme, meaning that any two NPUs are interconnected. The version of the Ascend Hardware Development Kit (HDK) is 23.0.2.1, and the version of the Compute Architecture for Neural Networks (CANN) suite is 7.0.0, which is the commercial release version for Q4 2023. The models in this paper use ModelLink, an LLM training framework based on the Ascend architecture, and run in the torch_npu 5.0.0 environment.

C.3 Model Configuration

This paper adopts the Mixtral $8 \times 7B$ model with an MoE structure, released in December 2023, as the backbone and embeds LocMoE and LocMoE+. Mixtral has 46.7B parameters and uses the Group Query Attention (GQA) mechanism to compute attention. It contains 32 sparse expert blocks, with the MoE Feedforward layer comprising 8 experts, and each token selects the top 2 experts for processing. In the application scenarios of this paper, the corpora are generally long texts; thus, the sequence length is adjusted to 32768. For the three cluster scales of 32N, 64N, and 256N, the parallel strategies are set as follows: 32N - tensor parallel (TP=4) / pipeline parallel (PP=4) / data parallel (DP=2) / expert parallel (EP=2), 64N - TP=8 / PP=4 / DP=2 / EP=2, and 256N - TP=8 / PP=8 / DP=4 / EP=2. The batch size is set to 128.

C.4 Evaluation Metrics and Datasets

To evaluate model performance, this paper designs a comprehensive metric called the General and Domain-specific Assessment Dataset (GDAD), which consists of three evaluation systems: domain

task capability, domain capability certification exam, and general capability. Among them, the domain task capability includes a total of 16 categories and 2,657 questions, such as domain logical reasoning; the domain capability certification exam includes a total of 13 categories and 13,968 questions, such as data communication; and the general capability includes a total of 18 categories and 1,435 questions, such as programming ability. The questions include objective and subjective questions in Chinese, English, and bilingual formats. For subjective questions, the cosine similarity between the model output and the standard answer is used as the score. In addition, this paper also employs C-Eval [40] and TeleQnA [41] to evaluate the model's Chinese language capability.